Progress In Electromagnetics Research C, Vol. 108, 13–22, 2021

Design of the Segmented-Type Switched Reluctance Linear Synchronous Motor (SSRLSM) for Domestic Lift Application

Nur A. M. Nasir[1, 2], Fairul A. A. Shukor[1, 2, *], Nor A. M. Zuki,[1, 2], and Raja N. F. K. R. Othman[1, 2]

Abstract—This paper proposes an SRLSM with segmental stator pole. The segmented SRLSM which is known as SSRLSM was designed for domestic lift application. The SSRLSM was designed to fulfill the design target requirement where the lift must be able to transport a maximum 200 kg payload. This payload requires a motor with more than 2000 N thrust force at rated power of 1.5 kW. The rated current is 2.5 A. However, for the excitation current, the maximum current is taken twice of the rated current which is 5.0 A. The design of the SSRLSM was completed in two stages. The first stage is to design the stator pole length, l_{st}, while the second stage is to design the stator pole thickness, t_{st}. The designed models were simulated with FEM software. The simulation results show that the highest thrust produced in first stage is 6773 N. The thrust is produced by the model with stator pole length, l_{st}, of 120 mm. Meanwhile, in the second stage, the model with the stator pole thickness, t_{st}, of 20 mm produced the highest thrust. The thrust obtained from the model is 6903 N. Based on the analysis, the final model was selected. The model has the stator pole length, l_{st}, and stator pole thickness, t_{st}, of 120 mm and 20 mm, respectively.

1. INTRODUCTION

Elevator, or also known as a lift, is a device that increases or decreases a person's potential energy without his/her needing to supply that energy themselves. This is because the elevator provides the potential energy of going up and takes the potential energy of coming down. Based on this working principle, an elevator requires a linear motion principle that can move up and down. Conventionally, a linear motion is produced by using motion translators to convert rotational motion to linear motion [1]. The examples of the commonly used motion translators are belts, gears, and ball screws. The conventional motion system introduces a few weaknesses such as low acceleration performance, mechanical complexity and limitation, backlash, and low impact load capacity [2]. In lift application, these disadvantages can cause mechanical complexity, and additional room is required to place the motor. To overcome this problem, a modern linear motion system that produces direct linear motion was introduced. This linear motion system eliminates motion translators resulted in a system that has a simple structure, high dynamic response, high speed, and high accuracy [3]. This motion system was produced by a linear motor instead of a rotational motor.

At present, linear synchronous motors (LSMs) have been proposed for the primary propulsion of vertical transportation systems [4–8]. LSMs can be divided into two types. They are switched reluctance linear synchronous motor (SRLSM) and permanent magnet linear synchronous motor (PMLSM). Compared to an SRLSM, a PMLSM has additional permanent magnets on its mover side. Therefore, it

Received 2 November 2020, Accepted 22 December 2020, Scheduled 31 December 2020

* Corresponding author: Fairul Azhar bin Abdul Shukor (fairul.azhar@utem.edu.my).

[1] Faculty of Electrical Engineering, Universiti Teknikal Malaysia Melaka (UTeM), Hang Tuah Jaya, Durian Tunggal, Melaka 76100, Malaysia. [2] Electrical Machine Design, Power Electronics and Drives Research Group, CeRIA, UTeM, Hang Tuah Jaya, Durian Tunggal, Melaka 76100, Malaysia.

has two magnetic sources that help to increase the thrust density of the PMLSM. Despite its superior performance, PMLSM suffers from thrust fluctuation, especially during low-speed operation. The thrust fluctuation is mainly due to the existence of cogging force [9]. Apart from that, the manufacturing cost of a PMLSM can increase rapidly as the prices of permanent magnets are high [10]. On the other hand, due to the absence of the permanent magnet on its structure, the SRLSM does not suffer from the cogging force and manufacturing price fluctuation [11]. The other advantages that an SRLSM has over the PMLSM are that the SRLSM has a simpler structure and can operate at high temperatures.

The application of a switched reluctance motor in an elevator system is not something new. In recent years, SRLSM is increasingly advocated as an alternative to other linear electrical motors such as linear induction motor (LIM) and PMLSM. This is caused by their simple and robust construction with concentric windings on only one side, which is stator or translator, and fault tolerance due to the absence of mutual coupling between windings, maintenance ease, less thermal problems and cooling arrangement, and finally low cost [12]. With these advantages, SRLSMs have been studied for their suitability in some linear applications such as in horizontal linear transportation systems, high-precision position application in manufacturing automation, and cylindrical type linear actuator using an SRLSM for applications requiring controlled low-speed linear motion [12].

2. SEGMENTED SWITCHED RELUCTANCE LINEAR SYNCHRONOUS MOTOR

In this research, an SRLSM is designed as a segmented-type. Compared to a conventional SRLSM, the segmented SRLSM was designed without teeth on both the mover and the stator sides. The purpose of the design topology is to reduce manufacturing tolerance as well as to increase the efficiency of motor performance.

2.1. Design Target

In a multilevel building, there is a regulation that requires the developer to provide an elevator to physically handicapped people especially in a building where it is impractical to construct and build a wheelchair ramp [13]. In Malaysia, there are a few Malaysian standard codes of practice on access for disabled persons that specify the basic requirement of buildings and related facilities to permit access for disabled persons [14]. Apart from a person with a wheelchair, an elevator can also help elderly people and obese people to easily move in a multistoried building.

In this research, an SSRLSM-based domestic lift was proposed in a laboratory scale for case study analysis. Figure 1 shows the skeleton of the proposed SSRLSM domestic lift. The domestic lift was designed based on specific design targets such as minimum thrust requirement, rated current, and rated power. The domestic lift was designed to be able to transport a maximum of two people at a time with a maximum payload; 2 people and luggage weigh 200 kg. Therefore, it requires a motor with more than 2000 N at rated power, P_{rated} of 1.5 kW to operate the lift. The rated current, I_{rated}, for the motor is 2.5 A. However, for the excitation current, I, the maximum current is taken twice of the rated current which is 5.0 A.

2.2. Basic Thrust Equation of the SSRLSM

When the coil of the SSRLSM is energized by a certain current, I, a magnetic flux, Φ, is induced and flows from the mover to the stator. The thrust of the SSRLSM is developed when the unaligned pole is attracted to each other until the aligned position is achieved. Figure 2 shows the relation between magnetic flux, Φ, and displacement, x.

Based on the flux profile shown in Figure 2, the magnetic flux, Φ, can be expressed as Fourier Series as in Eq. (1) [15].

$$\Phi = \Phi_{DC} + \sum_{n=1}^{\infty} \Phi_n \cos \frac{2\pi}{\tau_p} nx \,(\text{Wb}) \tag{1}$$

where Φ_{DC} is the DC component of magnetic flux in (Wb), n the Fourier order, Φ_n the nth Fourier component of magnetic flux in (Wb), τ_p the pole pitch in (m), and x the stator displacement in (m).

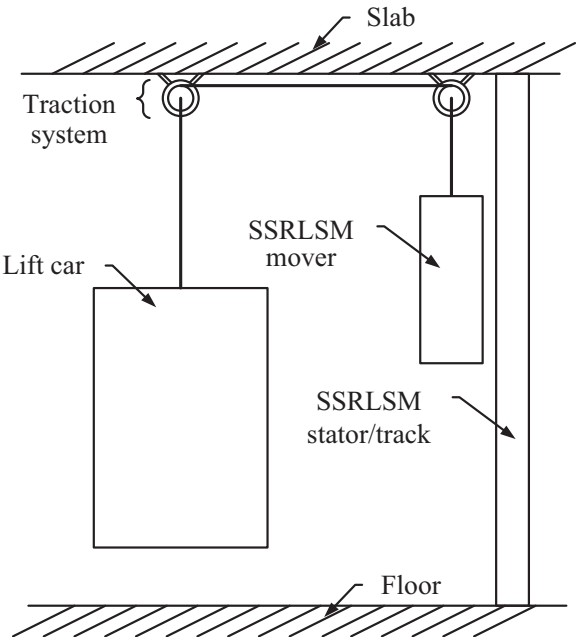

Figure 1. Skeleton of the SSRLSM domestic lift.

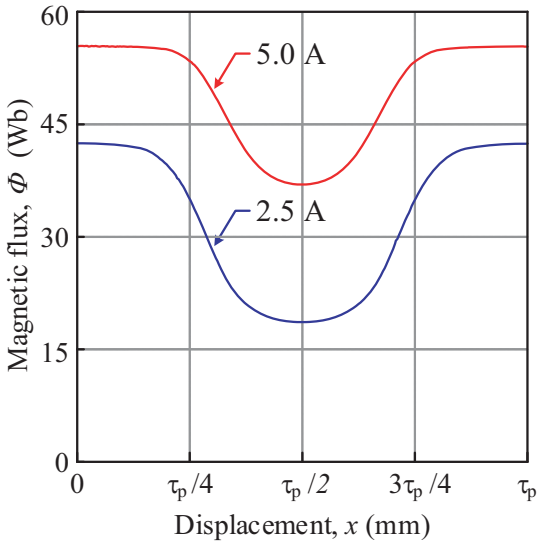

Figure 2. Magnetic flux, Φ.

The magnetic energy of the SSRSLM, W, can be calculated using Eq. (2).

$$\begin{aligned} W &= N\int_0^I \Phi dI \\ &= NI\Phi\,(\mathrm{J}) \end{aligned} \tag{2}$$

where W is the magnetic energy in (J), N the coil turn, Φ the magnetic flux expression in (Wb), and I the input current in (A).

Based on Eq. (1), the expression of magnetic energy, W, can be rewritten as Eq. (3).

$$\begin{aligned} W &= NI\left[\Phi_{DC} + \sum_{n=1}^{\infty}\Phi_n \cos\frac{2\pi}{\tau_p}nx\right] \\ &= NI\Phi_{DC} + \sum_{n=1}^{\infty} NI\Phi_n \cos\frac{2\pi}{\tau_p}nx\,(\mathrm{J}) \end{aligned} \tag{3}$$

The thrust, F, can be calculated by differentiating the magnetic energy, W, with respect to the mover displacement, x, as shown in Eq. (4).

$$\begin{aligned} F &= \frac{dW}{dx} \\ &= \frac{d}{dx}\left[NI\Phi_{DC} + \sum_{n=1}^{\infty} NI\Phi_n \cos\frac{2\pi}{\tau_p}nx\right]\,(\mathrm{N}) \end{aligned} \tag{4}$$

By solving the differentiation in Eq. (4), the general thrust for the SSRLSM can be expressed as Eq. (5) [15].

$$\begin{aligned} F &= -NI\sum_{n=1}^{\infty}\Phi_n \sin\left[\frac{2\pi}{\tau_p}nx\right]\cdot\frac{2\pi n}{\tau_p} \\ &= \frac{2\pi NI}{\tau_p}\sum_{n=1}^{\infty} n\Phi_n \sin\frac{2\pi}{\tau_p}nx\,(\mathrm{N}) \end{aligned} \tag{5}$$

Based on Eq. (5), despite coil parameter such as coil turns, N, and current, I, the thrust of the SSRSLM also depends on the pole pitch, τ_p.

3. DESIGNING SEGMENTED SWITCHED RELUCTANCE LINEAR SYNCHRONOUS MOTOR

Figure 3 shows the basic structure of the 3 phase 6-slot 4-pole SSRLSM. The SSRLSM is designed in a flat structure. The mover consists of yoke and coil. The stator side consists of stator track and segmental stator pole. The material for the stator pole and stator yoke is SS400. The stator track is made of aluminum.

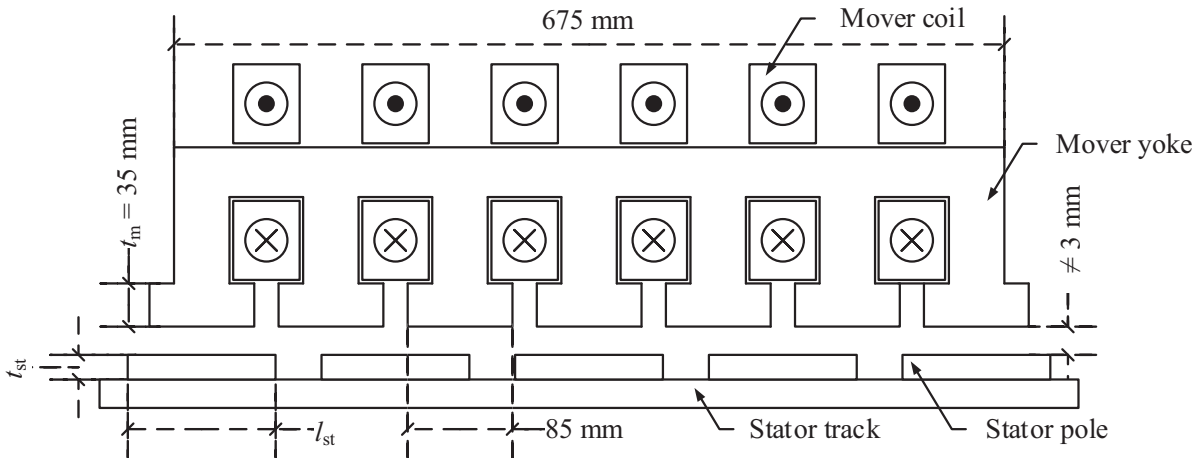

Figure 3. Basic structure of the SSRLSM.

In order to identify the optimum model for fabrication, two structure parameters were varied in the design modelling. They are stator pole length, l_{st}, and stator pole thickness, t_{st}. For both parameters, the values were varied starting from the lowest possible to the highest possible values. The modelling of each structure was designed with CAD software then simulated with FEM software. The FEM outputs were then analysed and compared to identify the model with the highest thrust, F.

Apart from the stator pole length, l_{st}, and stator pole thickness, t_{st}, the other structure parameters of the SSRLSM were fixed throughout the design process. The fixed parameters are stack length, L, air gap length, δ, mover shoe length, l_m, and mover shoe thickness, t_m. Table 1 shows the structure specification of the SSRLM designed for both design stages.

Figure 4 shows the SSRLSM design flowchart for both stages. For the first stage, the design started

Table 1. Specification of the proposed SSRLSM.

Parameter	Value
Stack length, L	400 mm
Air gap length, δ	3 mm
Mover shoe length, l_m	85 mm
Mover shoe thickness, t_m	35 mm
Stator pole length, l_{st}	60 mm $\sim$ 150 mm
Stator pole thickness, t_{st}	10 mm $\sim$ 100 mm
Number of turns, N	1800
Winding resistance, R	20 Ω

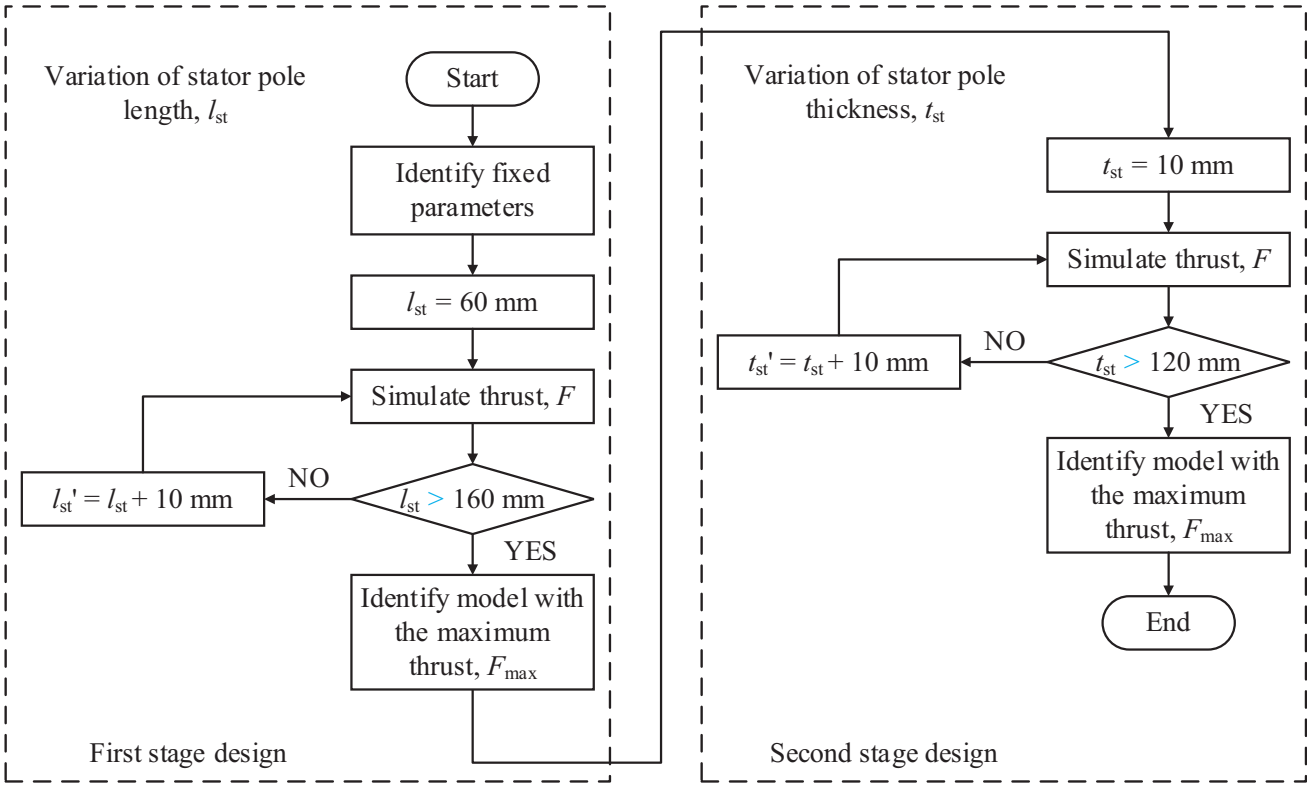

Figure 4. SSRLSM design flowchart.

by modelling the structure of the SSRLSM with different stator pole length, l_{st}, parameters with a fixed air gap, δ, and stator pole thickness, t_{st}. The stator pole length, l_{st}, was varied from 60 mm to 150 mm with 10 mm increment. Each model was simulated to obtain thrust characteristics. The simulation results were then compared in order to determine the model with the highest maximum thrust, $F_{\max}$.

Once the model with the highest maximum thrust, $F_{\max}$, has been identified, the SSRLM design was continued in the second stage. In the second stage, the stator pole length, l_{st}, of the chosen model in the first stage was taken and fixed throughout the design process. In this second stage, the stator pole thickness, t_{st}, was varied from 10 mm to 100 mm with 10 mm increment. Each model was simulated to obtain thrust characteristics. The simulation results were then compared in order to determine the model with the highest maximum thrust, $F_{\max}$.

4. PERFORMANCE OF THE SSRLSM

The SSRLSMs for different values of the stator pole length, l_{st}, and stator pole thickness, t_{st}, are designed and simulated with FEM software. Based on FEM results, their characteristics are compared and analyzed. The analysis involves magnetic flux analysis, thrust characteristics, and total harmonic distortion for thrust, THD_F.

4.1. Magnetic Analysis

Figure 5 shows the magnetic flux lines analysis of Phase B SSRLSM for both fully aligned and fully unaligned positions. In the SSRLSM, when the coil is excited, it will induce the magnetic flux where the flux will flow from the mover yoke to the stator pole by passing through the air gap to complete a closed path. The magnetic flux lines in Figure 5 show that the magnetic lines are more concentrated on the mover yoke when a higher current is injected into the coil.

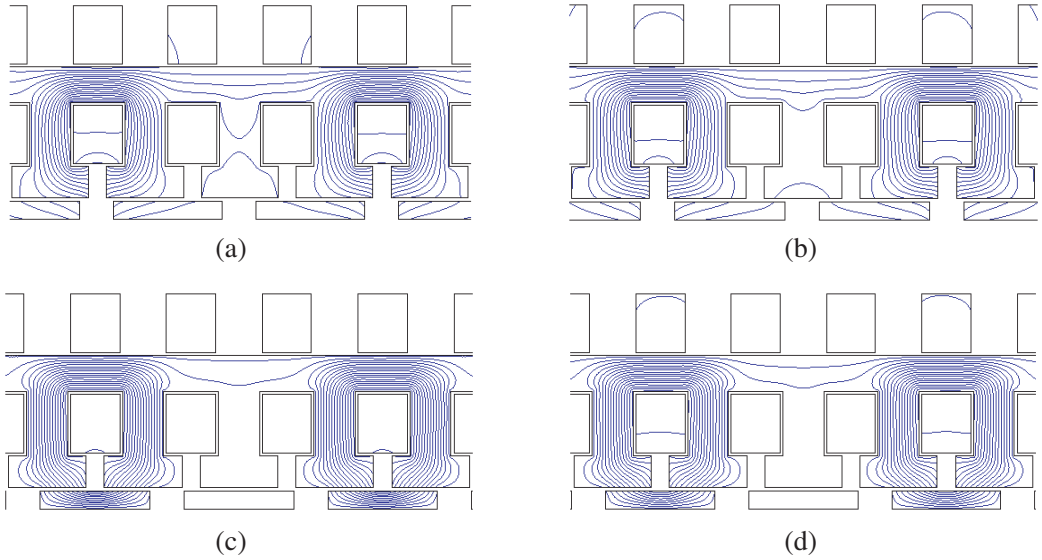

Figure 5. Magnetic flux line. (a) Fully unaligned ($I = 2.5\,\mathrm{A}$). (b) Fully unaligned ($I = 5.0\,\mathrm{A}$). (c) Fully aligned ($I = 2.5\,\mathrm{A}$). (d) Fully aligned ($I = 5.0\,\mathrm{A}$).

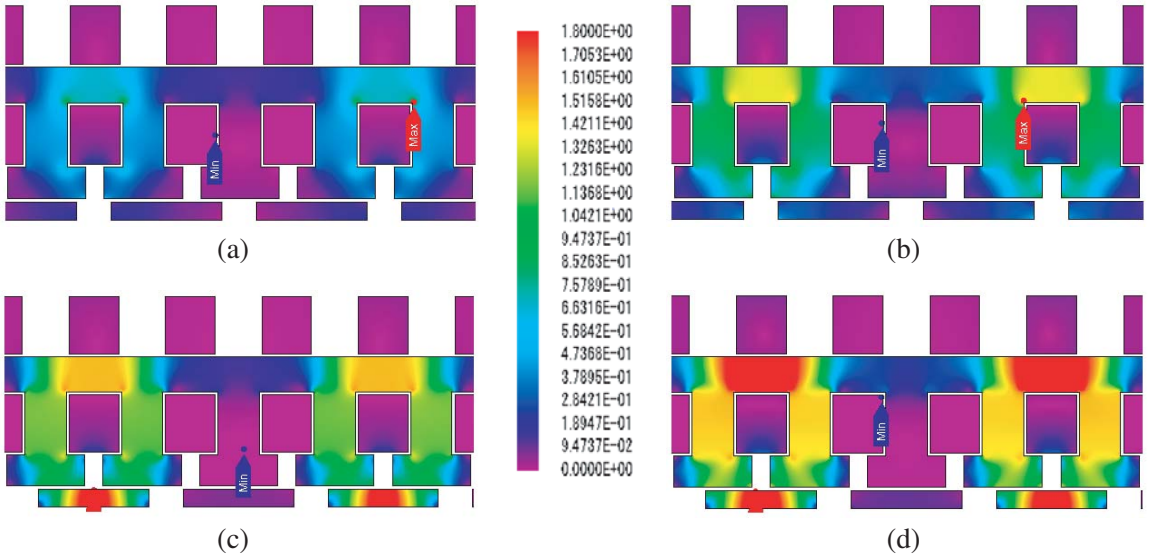

Figure 6. Magnetic flux density, $\boldsymbol{B}$. (a) Fully unaligned ($I = 2.5\,\mathrm{A}$). (b) Fully unaligned ($I = 5.0\,\mathrm{A}$). (c) Fully aligned ($I = 2.5\,\mathrm{A}$). (d) Fully aligned ($I = 5.0\,\mathrm{A}$).

Figure 6 shows the magnetic flux density, $\boldsymbol{B}$, distribution for the SSRLSM. The indigo colour shows the regions where the magnetic flux density, $\boldsymbol{B}$, is minimum. Oppositely, the red regions are the region with maximum magnetic flux density, $\boldsymbol{B}$. In Figures 6(a) and (b), it can be observed that the magnetic flux density, $\boldsymbol{B}$, is mostly concentrated in the upper region of the mover yoke. At the fully unaligned position, the maximum magnetic flux densities, $\boldsymbol{B}$, recorded at given currents of 2.5 A and 5.0 A are 1.09 T and 1.62 T, respectively. Meanwhile, the minimum magnetic flux density, $\boldsymbol{B}$, at both given current is nearly 0 T. Nevertheless, at the fully aligned position, the magnetic flux density, $\boldsymbol{B}$, observed at excitation current is higher at the stator pole area. In this condition, the maximum 1.8 T was recorded at the stator pole. The same condition can be observed at higher current, I, of 5.0 A where the magnetic flux density, $\boldsymbol{B}$, is intensified at both upper region of mover yoke and stator pole where

1.8 T is obtained. Overall, it can be observed that magnetic flux density, $\boldsymbol{B}$, distribution is higher at a fully aligned position.

4.2. Variation of the Stator Pole Length, l_{st}

Figure 7 shows the thrust, F, of the SSRLSM at the input current, I, of 5.0 A. The thrust characteristics shown are for the different values of stator pole length, l_{st}. Based on the thrust characteristics shown in Figure 7(a), the maximum thrust, $F_{\max}$, for each stator pole length, l_{st}, is identified. The maximum thrust, $F_{\max}$, is shown in Figure 7(b). The thrust pattern shows that as the stator pole length, l_{st}, increases from 60 mm to 120 mm, the thrust, F, obtained increases. However, starting from stator pole length, l_{st}, 130 mm to 150 mm, the produced thrust decreases. The highest thrust, F, produced is identified from the model with the stator pole length, l_{st}, of 120 mm. The maximum thrust, $F_{\max}$, of the model is 6773 N. Apart from the thrust characteristics, the other performance observed in this SSRLSM design is the total harmonic distortion of thrust, THD_F. In the SSRLSM, a lower THD_F has a better thrust performance. This is because the thrust with lower THD_F has lower thrust ripple. Therefore, the thrust with a lower thrust ripple has a waveform near a sinusoidal shape. In order to determine THD_F of the SSRLSM, THD_F was calculated based on the thrust, F, characteristics, obtained by using Eq. (6). The calculated THD_F was plotted in Figure 7(b). Overall, it shows that THD_F is inversely proportional to the stator pole length, l_{st}. The model with the stator pole length, l_{st}, of 60 mm has the highest THD_F which is 147.97%. The lowest THD_F calculated is 34.45% which is produced by the model with the stator pole length, l_{st}, of 110 mm.

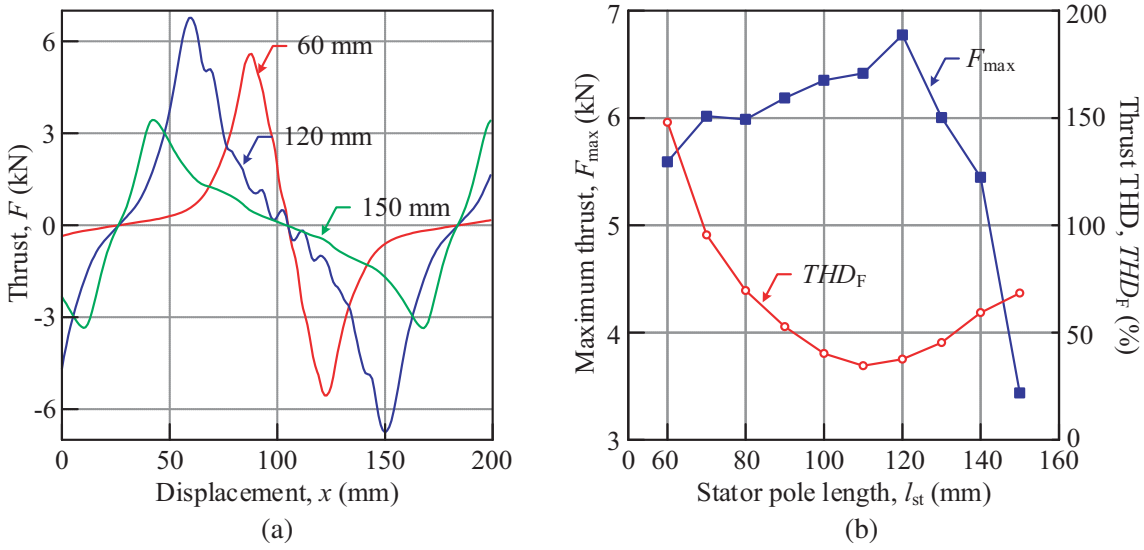

Figure 7. Thrust characteristic for different stator pole length, l_{st}. (a) F ($I = 5.0$). (b) $F_{\max}$, THD_F ($I = 5.0$ A).

4.3. Variation of the Stator Pole Thickness, t_{st}

Figure 8 shows the thrust characteristics of the SSRLSM for different values of stator pole thickness, t_{st}. The thrust, F, was taken at the excitation current, I, of 5.0 A. Based on the thrust characteristics shown in Figure 8(a), the maximum thrust, $F_{\max}$, for each stator pole thickness, t_{st}, is identified. The identified maximum thrust, $F_{\max}$, is shown in Figure 8(b). It shows that the thrust is increased until it reaches its maximum value before it is reduced. The highest thrust, F, obtained in this stage is from the model with the stator pole thickness, t_{st}, of 20 mm. The maximum thrust, $F_{\max}$, of this model is 6903 N. The total harmonic distortion for thrust, THD_F, obtained also shows that it is in an inverse relationship with the stator pole thickness, t_{st}. The highest THD_F is produced by the model with the

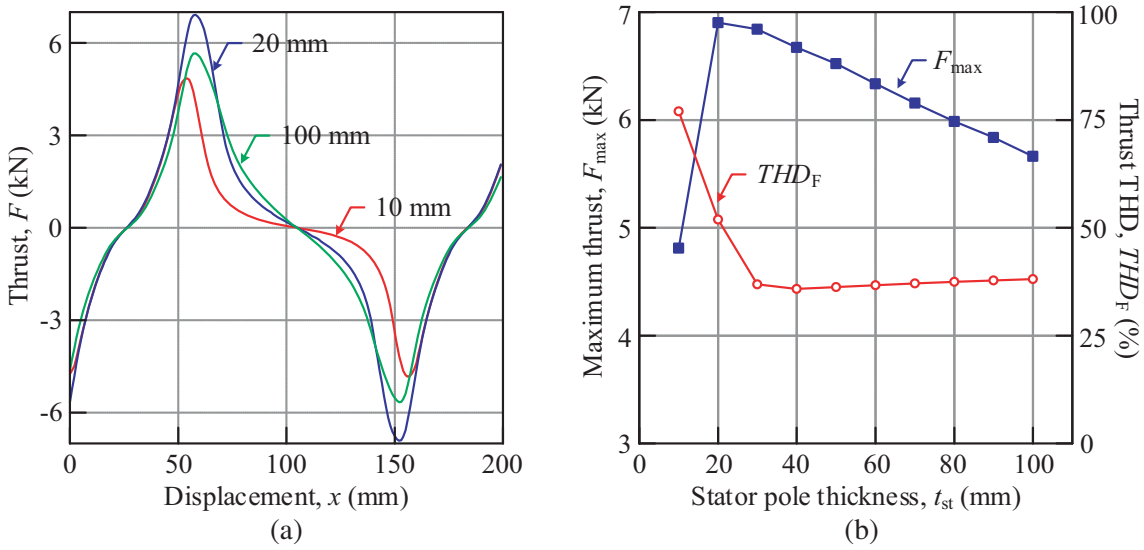

Figure 8. Thrust characteristic for different stator pole thickness, t_{st}. (a) F ($I = 5.0$). (b) $F_{\max}$, THD_F ($I = 5.0$ A).

stator pole thickness, t_{st}, of 10 mm which is 77%. Oppositely, the lowest THD_F is produced by the model with the stator pole thickness, t_{st}, of 40 mm. THD_F produced by the model is 35.82%.

4.4. Final Structure Parameters of the SSRLSM

Basically, based on the thrust characteristics of the SSRLSM designed in both stages, the best model was selected in each stage. The model was selected based on the highest maximum thrust, $F_{\max}$, produced. The specification and performance of the selected model in each stage are shown in Table 2. Table 2 shows that the model selected in the second stage has a higher thrust, F, than the model selected in the first stage.

Table 2. Specification of the selected models.

	First stage design		Second stage design	
Parameters chosen	Parameter	Value	Parameter	Value
	Stator pole length, l_{st}	120 mm	Stator pole length, l_{st}	120 mm
	Stator pole thickness, t_{st}	60 mm	Stator pole thickness, t_{st}	20 mm
Maximum thrust, $F_{\max}$(% increment)	6773 N		6903 N (+1.92%)	
Total harmonic distortion of thrust, THD_F (% increment)	37.61%		51.89% (+57.2%)	

Based on this finding, it is decided that the selected model in the second stage is the most optimum model to be fabricated. The final structure and specification of the proposed SSRLSM are shown in Figure 9 and Table 3, respectively. The stator pole length, l_{st}, and stator pole thickness, t_{st}, of the SSRLSM of the selected model are 20 mm and 120 mm, respectively. At the excitation current of 5.0 A, the model produced the maximum thrust, $F_{\max}$, of 6903 N. As the final model has been selected, the maximum thrust, $F_{\max}$, for each given current of the model was identified and is shown in Figure 9.

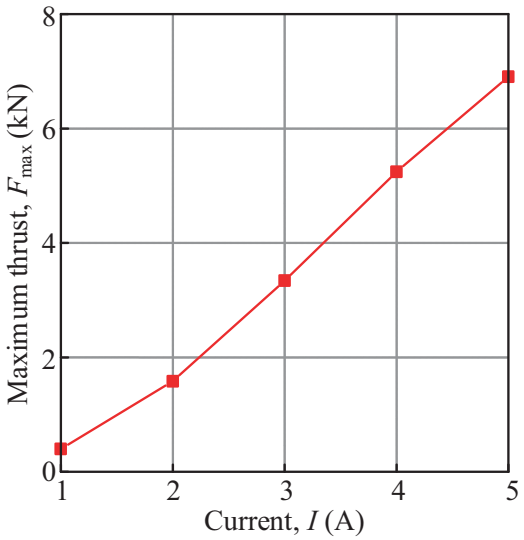

Figure 9. Thrust characteristics of the final model.

Based on the thrust characteristics, it is shown that at excitation current of 2.5 A (rated current), the thrust produced already fulfilled the design target requirement.

5. CONCLUSION

The SSRLSM for the domestic lift application has been designed. The design of the SSRLSM was completed in two stages. Based on the simulation results, it is shown that the maximum thrust, $F_{\max}$, produced by the selected model in the second stage increased by almost 2% from the model selected in the first stage design. Therefore, it is decided that the specification of the model chosen in the second stage design will be used in the model to be fabricated. The model has the maximum thrust, $F_{\max}$, of 6903 N at the current, I, of 5.0 A. At the given current, I, of 5.0 A, the magnetic analysis shows that the model has the magnetic flux, Φ, of 55 Wb with the magnetic flux density, $\boldsymbol{B}$, of 1.8 T. Based on the SSRLSM performance, it can be concluded that the designed SSRLSM fulfilled the design target requirement for the lift application. Therefore, the SSRLSM will be fabricated for further research analysis.

ACKNOWLEDGMENT

The authors would like to thank Ministry of Education Malaysia, Universiti Teknikal Malaysia Melaka (UTeM) for providing the research grant FRGS/2018/FKE-CERIA/F00356.

REFERENCES

1. Wu, Z. and Y. Xiang, "Linear rotary converter. A new technology for sea wave application," *2017 OCEANS*, 1–5, 2017.
2. Huang, Y., S. Zhou, G. Bao, and Z. Wang, "Design and optimization for unilateral flat permanent linear motor," *CSAE 2012 — Proceedings, 2012 IEEE International Conference on Computer Science and Automation Engineering*, Vol. 1, 687–691, 2012.
3. Hirayama, T., T. Hiraishi, and S. Kawabata, "Study on transfer system with both long-distance driving and high positioning accuracy using linear switched reluctance motor," *2016 19th International Conference on Electrical Machines and Systems (ICEMS)*, 1–4, 2016.

4. Masoudi, S., M. B. Banna Sharifian, and M. R. Feyzi, "Force ripple and jerk minimisation in double sided linear switched reluctance motor used in elevator application," *IET Electric Power Applications*, Vol. 10, No. 6, 508–516, 2016.
5. Wang, D. H., X. H. Wang, C. L. Shao, and Z. L. Wang, "Analysis and design of an annular winding dual side stator linear switch reluctance machine for ropless elevator driving system," *2015 IEEE International Conference on Applied Superconductivity and Electromagnetic Devices (ASEMD)*, 322–323, 2015.
6. Fernandez, J. R. and P. Cortez, "A survey of elevator group control systems for vertical transportation: A look at recent literature," *IEEE Control Systems Magazine*, Vol. 35, No. 4, 38–55, 2015.
7. Anand, R. and M. Mahesh, "Vertical transportation: an overview on system integration with advance technology," *2017 International Conference on Smart Technologies for Smart Nation (SmartTechCon)*, 476–479, 2017.
8. Wang, D., X. Du, D. Zhang, and X. Wang, "Design, optimization, and prototyping of segmental-type linear switched-reluctance motor with a toroidally wound mover for vertical propulsion application," *IEEE Transactions on Industrial Electronics*, Vol. 65, No. 2, 1865–1874, 2018.
9. Oshima, S., S. Tahara, and K. Ogawa, "Thrust and thrust ripple of linear reluctance motor compared permanent linear synchronous motor," *15th Inter. Conf. on Electrical Machine and Systems (ICEMS) 2012*, 1–4, 2012.
10. Yoon, K. and B. Kwon, "Optimal design of a new interior permanent magnet motor using a flared-shape arrangement of ferrite magnets," *IEEE Transactions on Magnetics*, Vol. 52, No. 7, 1–4, 2016.
11. Ding, K., "The rare earth magnet industry and rare earth price in China," *EPJ Web of Conferences*, Vol. 5, No. 04005, 2014.
12. Mecrow, B. C., J. W. Finch, E. A. El-Kharashi, and A. G. Jack, "Switched reluctance motors with segmental rotors," *IEE Proc. — Electr. Power Appl.*, Vol. 149, No. 4, 245–254, 2002.
13. Anand, R. and M. Mahesh, "Analysis of elevator drives energy consumptions with permanent magnet machines," *2016 IEEE Smart Energy Grid Engineering (SEGE)*, 186–190, 2016.
14. Kamarudin, H., N. R. Muhamad Ariff, W. Z. Wan Ismail, A. F. Bakri, and Z. Ithnin, "Malaysian scenario on access and facilities for persons with disabilities: A literature review," *MATEC Web of Conferences*, Vol. 15, No. 01019, 2014.
15. Yamamoto, Y. and H. Yamada, "Analysis of magnetic circuit and starting characteristics of flat-type linear pulse motor with permanent magnets," *T. IEE Japan*, Vol. 104-B, No. 5, 265–272, 1984.